Role of Impurity Nanoparticles in Laser-Induced Nucleation of Ammonium Chloride

On the role of impurity nanoparticles in laser-induced nucleation of ammonium chloride

Martin R. Ward, Alasdair M. Mackenzie, Andrew J. Alexander*

School of Chemistry, University of Edinburgh, Edinburgh, Scotland, EH9 3FJ

Abstract

Results of experiments on laser-induced nucleation (LIN) in supersaturated (S = 1.20) aqueous ammonium chloride solutions are presented. Measurement of the particle-size distribution in unfiltered solutions near saturation (95%) indicates a population of nanometer-scale species with mean hydrodynamic diameter 750 nm, which is almost entirely removed by single-pass filtration through a poly(ether sulfone) membrane (0.2 μm pores). Analysis of filter residues reveals iron and phosphate as major impurities in the solute. Experiments show that the number of nuclei induced by LIN can be reduced substantially by pre-processing (filtering or long-term exposure to laser pulses) and that this reduction can be reversed by intentional doping with iron-oxide (Fe_3O_4) nanoparticles. The use of surfactant to assist dispersion of the nanoparticles was found to increase the number of laser-induced nuclei. We discuss the results with reference to mechanisms of non-photochemical laser-induced nucleation (NPLIN).

1. Introduction

The process of nucleation is of fundamental scientific interest, and is a key step in the production of high-value solid materials, such as pharmaceuticals and agrochemicals. The stochastic nature of nucleation makes experimental and theoretical studies of nucleation dynamics very challenging. The advent of pulsed-laser methods, however, has opened up new possibilities to explore nucleation mechanisms in detail. Laser-induced nucleation (LIN) may be classed as photochemical or non-photochemical. In photochemical LIN, reactive species are formed, such as ions or radicals, which can cause aggregation of solute molecules and production of nuclei.[1-2] Non-photochemical LIN (NPLIN) generally requires relatively lower intensities of light at wavelengths where there are no strong absorption bands in the system; short, unfocussed pulses (ps to ns) of laser light are typically used. Systems that have been studied using NPLIN include small molecules such as glycine and carbamazepine,[3-9] simple salts such as KCl,[10-12] single-component systems such as acetic acid and sodium chlorate,[13-14] and large molecules such as proteins.[15-16] The main advantage of NPLIN is that it appears to be similar to homogeneous

nucleation: it requires only solute and solvent, occurs in the bulk of the solution, and there is no chemical damage to molecules. A variant of NPLIN based on optical trapping using continuous-wave laser light has been demonstrated;[17-18] in the remainder of this article, however, we will deal specifically with pulsed laser-induced nucleation.

Up to now, the mechanism for NPLIN is believed to involve the interaction between the electric field (***E***) of the laser pulse, and the polarizability of solute molecules in clusters. For nucleation of simple salts from solution, the interaction of the transient *E*-field with a sub-critical cluster acts to lower its free energy, causing a change in its structure.[10, 12] In the case of small molecules, the difference in polarizability along different directions of the molecule means that molecules can become aligned with respect to the direction of the *E*-field, analogous to the optical Kerr effect (OKE).[5, 19] The resulting increase in structural order due to the interaction between the *E*-field and solute cluster gives rise to nucleation.

There are several pieces of evidence that support the polarizability mechanism for NPLIN. For example, it was observed that the nucleation probability is linearly proportional to E^2, as expected for the OKE.[12, 20] Needle-like crystals of urea that were nucleated by NPLIN were observed to be aligned with the electric field vector of linearly polarized light.[3] In the cases of glycine and of L-histidine it was possible to control the product polymorph by use of circular versus linear polarized light.[4, 7] Garetz and co-workers found that supersaturated solutions of small molecules required an aging period of one or more days, which they attributed to time required for clusters of solute to form.[3, 7, 19] Aging was not required for halide salts, which may indicate that these clusters form more rapidly.[10, 12]

There are several unresolved issues with the polarizability mechanism, as summarized recently by Agarwal and Peters.[21] The observation of a minimum power required for nucleation at low laser powers is not readily explained. Moreover, the magnitude of the polarization interaction energy ($\sim 10^{-4}\ k_B T$) is very low compared to the background thermal energy, so that any structural ordering due to the electric field would be washed out, even if co-operative effects within a cluster are taken into account.[22-23] A phenomenological model of NPLIN based on pre-nucleating metallic clusters can account for some of these anomalies,[24] although it is not clear if this model is applicable to dielectric solutes.

Knott et al. conducted experiments on aqueous solutions of carbon dioxide, using the same laser pulse powers and pulse widths as experiments on NPLIN of solids, and showed that nucleation of CO_2 bubbles was possible.[25] No significant difference between carbonated tap water

and carbonated ultrapure water was observed, suggesting that impurities were not involved. It was argued that the results could not be explained by the polarizability mechanism, since the product phase is less dense and has a lower refractive index. Knott and co-workers discussed a range of possible alternative NPLIN mechanisms, including photochemistry resulting from weak absorption bands, or microscopic bubble cavitation. In a detailed study on LIN of carbon dioxide bubbles in carbonated sugar solutions, Ward et al. found that the number of bubbles nucleated was linearly proportional to sucrose concentration.[26] Filtered samples were shown to produce substantially fewer bubbles. Experiments on carbonated water showed that increasing degrees of cleaning and filtering during sample preparation reduced the number of bubbles observed. Ward et al. found it was not possible to switch off LIN completely, which they attributed to the difficulty in producing entirely clean, bulk solutions. The threshold power for LIN of bubbles (~4.7 MW cm^{-2}) was found to be very similar to previous work on NPLIN of alkali halides (~5.2 MW cm^{-2}).[12] The results suggested that impurity particles are required for LIN of bubbles. The findings were explained using a simple model based on heating of solid nanoparticles, which cause vapor bubbles to form and act as nuclei for bubble growth.[26]

In previous studies of NPLIN of KCl, it was noted that unfiltered samples were significantly more labile than filtered samples.[10] Because LIN was observed even when great care was taken to exclude dust and impurities, it was considered that presence of impurities was not a necessary condition for the effect. By carefully separating spontaneous from laser-induced nucleation events over time, Javid et al. have recently demonstrated that filtration suppresses NPLIN in aqueous glycine.[27] The work on CO_2 bubble nucleation suggests that it is not possible to remove potentially active impurity particles entirely, even with careful procedures.[26] In this article, therefore, we evaluate the role of impurity particles on LIN of crystals from solution.

2. Experimental

2.1 Laser-induced nucleation

Aqueous supersaturated solutions of ammonium chloride were used for experiments. Nucleation and growth of crystals in these samples occurs visibly within seconds, which allows easy discrimination between spontaneous nucleation and laser-induced nucleation. Sample vials used in all experiments were thoroughly cleaned using warm soapy water, and rinsed several times with filtered water before use. Ultrapure water (18.2 MΩ cm) was obtained from a water purification system (Sartorius arium comfort I); the ultrapure water was used for cleaning

glassware and preparation of sample solutions. The saturation concentration (molality) of aqueous ammonium chloride solution at 22 °C (C_{sat}) was 7.16 mol kg^{-1}.[28] A solution of concentration, C = 8.60 mol kg^{-1}, was prepared by dissolution of solid (Sigma-Aldrich 213330, batch number BCBM1220V) in ultrapure water, giving a resulting supersaturation, $S = C / C_{sat}$ = 1.20. Complete dissolution was ensured by the use of a water bath held at 45 °C, over the period of about 1 hour, with manual shaking of the solution every few minutes. When fully dissolved, warm solution was transferred to pre-cleaned sample vials (4 mL, 14.8 mm diameter) which were then sealed immediately. Filtered solution samples were prepared by filtering warm solution (45 °C) through syringe filters [0.22 µm, Millex GP, poly(ether sulfone) membrane]. Syringes were pre-warmed, but filters were not. The manufacturer's recommended maximum operating temperature for the filters was 45 °C. The remaining solution was used for laser processing (section 2.2).

Sample solutions were intentionally crystallized by cooling, and stored until required. These solutions were dissolved by gentle heating on a hot plate (40–50 °C) for 1 hour (with periodic shaking) and then cooled slowly to room temperature (22 °C), first in air and then using a water bath. We found that undisturbed samples generally remain supersaturated for several days or weeks; unfiltered samples are more liable to spontaneous nucleation. After a cooling period of 40 minutes, samples were removed and exposed to single pulses of light (1064 nm, full width at half-maximum of 5.5 ns) from an Nd^{3+}:YAG laser (Quantel Brilliant). The laser-beam diameter was reduced from 7.5 to 3 mm using a Galilean telescope. The incident mean power was controlled by passing the beam through a Glan-laser polarizer whose transmission axis was rotated with respect to the axis of linear polarization of the laser. An incident mean laser power of 30 mW (measured at 10 pulses s^{-1}) was used in nucleation experiments. The cylindrical shape of the vial causes slight focusing of the beam, which we calculate by ray tracing. By taking averages of the values at the front and back of the vial, we calculate the average peak pulse power j_{peak} = 12 MW cm^{-2}, and energy density u = 700 J m^{-2}. Samples were exposed to 3 or fewer laser pulses, with an interval of 10 seconds between each pulse, until nucleation had occurred.

Videos of nucleation experiments were captured using a CCD camera (AVT Stingray F-033B) and a macro zoom-lens (Computar MLH-10X). The sample vials were illuminated by an external white-light source. Camera settings were adjusted to ensure good contrast between emerging crystals and the background. For samples that nucleated during laser irradiation, video

images were used to count the number of crystals produced for each nucleated sample. Examples of images recorded are shown in Figure 1.

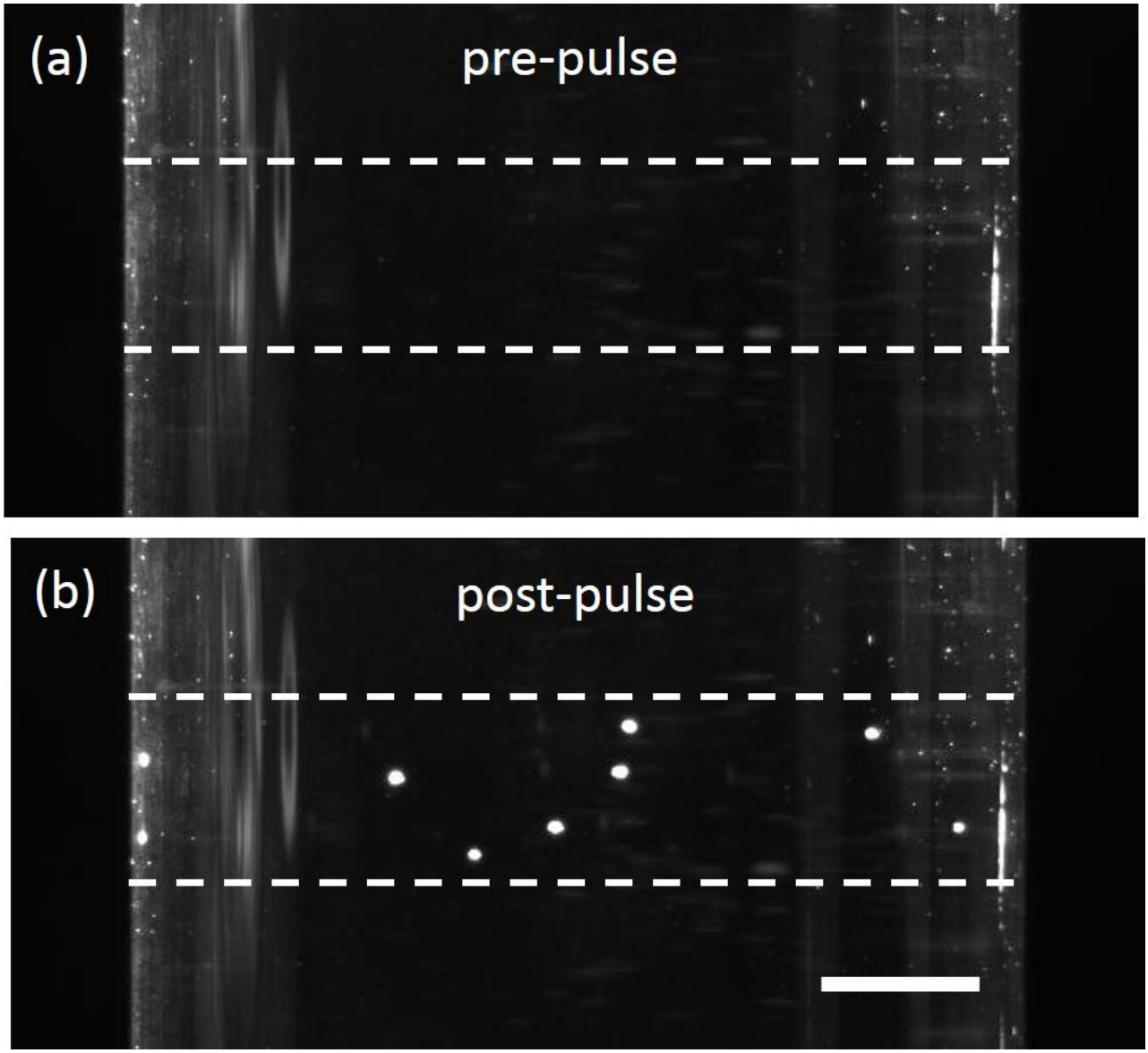

Figure 1. Images taken from video that show an unfiltered NH_4Cl solution (a) before, and (b) approximately 1.6 s after, nucleation by a single laser pulse. The images have been cropped to the region of interest, and the contrast has been enhanced to clearly discriminate nuclei. The path of the laser beam through the solution is indicated by the dashed white lines. Scale bar represents 2.5 mm.

2.2 Laser processing

To test if the laser is capable of destroying impurity particles that cause LIN, exposure to high intensity laser pulses over long periods was used. After preparation of the samples in vials, batches of the remaining stock ammonium chloride solution (approximately 100 mL) of molality

C = 8.60 mol kg^{-1} were irradiated at 10 pulse s^{-1} for periods of 30 or 120 minutes, with continuous stirring. The incident laser beam measured 6.5 mm in diameter and had a mean power of 1.9 W, which was the maximum power available from the laser. In order to avoid spontaneous or laser-induced nucleation of the solution, each batch was held at approximately 50 °C. Samples in vials were prepared from the laser processed solution, and tested for LIN using the same methods as outlined in section 2.1.

2.3 Solutions doped with nanoparticles

In order to produce samples doped with known amounts of solid nanoparticles, a stock solution of NH_4Cl of concentration C = 8.90 mol kg^{-1} was prepared and filtered into cleaned vials. A known quantity (~0.1 g) of liquid dopant was added to each vial to give a resulting concentration of C = 8.60 mol kg^{-1}. Three sets of 10 samples with different dopants were prepared. The liquid dopants included aqueous dispersions of iron-oxide nanoparticles (>98+%, Sigma 637106, LOT 11529AC, 20–30 nm nominal diameter), with and without poly(ethylene glycol) [PEG] surfactant (Fluka, 89510), and pure water as a control. Dispersions were placed in an ultrasonic bath for a period of one hour before use to ensure maximal dispersal. Details of the preparation of the nanoparticle dispersion can be found in the Supporting Information. All samples were tested for LIN following the procedures outlined in section 2.1.

3. Results

3.1 Effect of filtration

The number of primary nuclei produced per sample vial was counted from the video recorded during experiments. The results show a stark difference in the probability of LIN between filtered and unfiltered samples. It was found that 17 out of 26 filtered samples nucleated, giving a sample nucleation probability p = 0.65. In contrast, all 24 unfiltered samples were nucleated by the laser (p = 1.0). Filtered samples on average produced 1.4 ± 0.4 nuclei, whereas unfiltered samples produced 7.8 ± 1.3 nuclei (Figure 2). These results highlight the significant role that filtration plays in controlling the probability of LIN, and suggest that filtration acts to remove objects that are important to the mechanism.

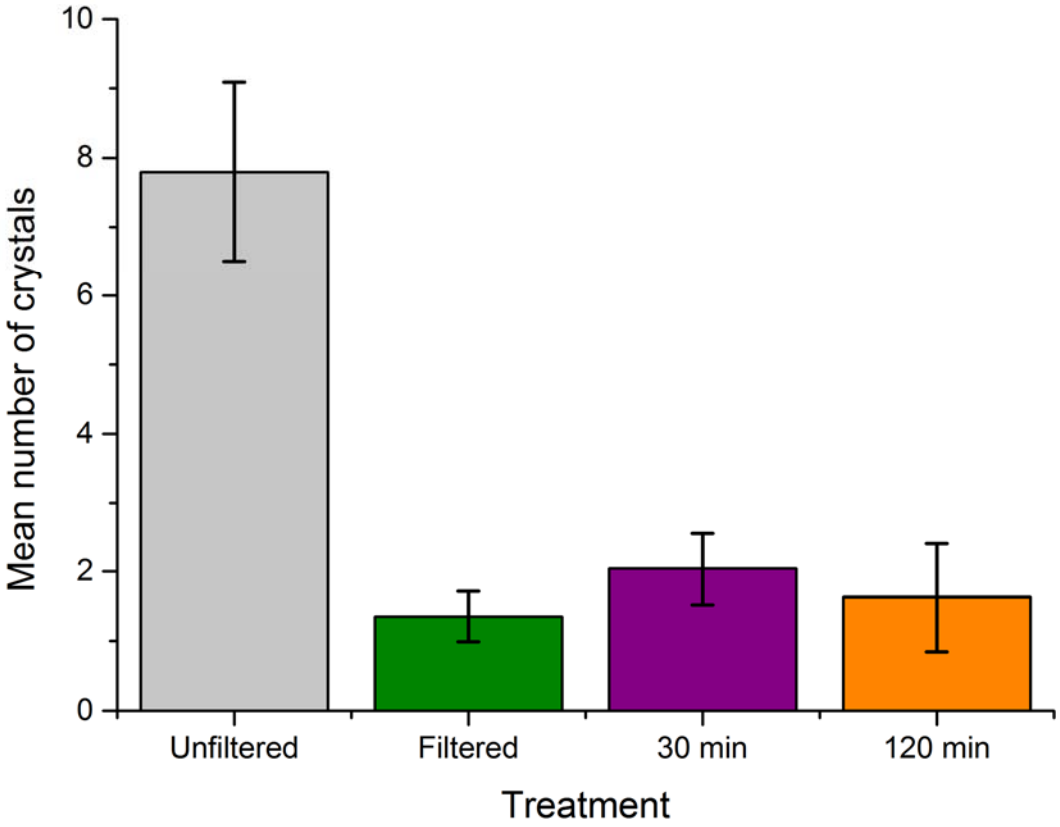

Figure 2. Graph showing the mean number of crystals produced by LIN for solutions that received different treatments before testing. Filtered samples (green bar) showed a greatly reduced number of crystals compared to unfiltered samples (grey bar). Unfiltered solution that was pre-processed by the laser for 30 minutes (purple bar) and 120 minutes (orange bar) produced an average number of crystals very similar to the filtered samples. Error bars represent 95% confidence limits for the mean.

3.2 Analysis of filter membrane

During filtration of concentrated ammonium chloride solution, it was observed that the filter membrane became lightly discolored (light-brown/orange color). Discoloration could be seen after passing approximately 40 mL of solution. To identify the chemical composition of the residue, a series of analyses were performed using inductively coupled-plasma optical-emission spectroscopy (ICP-OES) and mass spectrometry (ICP-MS). ICP-OES measurements indicated iron as the major component in the isolated residue with a concentration of 0.44 mg kg^{-1} (i.e., per kg of the NH_4Cl solid). The ICP-MS results also showed phosphorus as a major component, with an estimated concentration of 0.17 mg kg^{-1}. Details of the ICP-OES/MS sample preparation and a table of results is given in the Supporting Information. The results are consistent with the batch analysis obtained from the manufacturer, which certified Fe < 2 mg kg^{-1} and phosphate < 20 mg kg^{-1}.

The analysis suggests that filtration removes trace insoluble impurities, such as iron phosphate, from the sample solution. These impurities are present in the solid that was used to prepare the sample solution, with some particles small enough to pass through the 0.22-μm filters. Iron phosphate is a solid that is classed as insoluble in water with a yellow-brown color for both the Fe(II) and Fe(III) forms. Considering the stoichiometry of $Fe_3(PO_4)_2$ and $FePO_4$ an elemental ratio Fe/P of 1.5 or 1.0 would be expected, respectively. The concentrations measured from ICP experiments give an elemental ratio of 1.5 in the collected residue, which is the value for iron(II) phosphate.

3.3 Effect of laser processing

As described in section 2.2, laser processing was carried out to determine the effects of long-term exposure of solutions to laser pulses. The nucleation probability of processed solution was compared to that of unprocessed, unfiltered samples. When the solution was processed for 30 minutes, the measured nucleation probability (p = 24/27 = 0.89) was marginally lower compared to unprocessed solution (p = 1.0). The average number of nuclei produced from processed solution (2.0 ± 0.5) was, however, significantly lower compared to unprocessed solution (7.8 ± 1.3). When samples of solution were processed for a longer period (120 minutes), the nucleation probability (p = 19/19 =1.0) was the same as unprocessed, but the average number of nuclei formed (1.6 ± 0.4) was found to be slightly lower. The observed nucleation probabilities indicate that processed samples remain labile to LIN, but produce fewer nuclei.

The results of processing suggest that the laser destroys impurity particles. For nanoparticles that absorb laser light strongly, it is known that heating can lead to melting and possibly fragmentation.[29-30] Laser processing could reduce the size of impurity particles, leading to fewer large particles, and a corresponding relative reduction in the number of nuclei produced during LIN at a specific laser power.

3.4 LIN in doped samples

Our experiments show that it is possible to reduce the number of nuclei produced during LIN by removing some type of particles from solution. These particles could be clusters of solute, as discussed in section 1. However, ICP-OES/MS analyses show a significant concentration of Fe and phosphate in residues obtained by filtration of sample solution (section 3.2), which suggest that insoluble impurity nanoparticles are responsible for LIN. To test this hypothesis, we

investigated intentional doping of solutions with solid nanoparticles. Iron phosphate nanoparticles are typically produced by flame spray pyrolysis, which requires special expertise to produce homogeneous particles. For the present study, therefore, a series of filtered samples were intentionally doped with iron-oxide (Fe_3O_4) nanoparticles to mimic the impurities.

The results of LIN in doped NH_4Cl solutions are summarized in Figure 3. It was found that the nucleation probability (p = 6/10 = 0.6) and average number of nuclei produced per nucleated sample (1.0 ± 0.0) for control samples (pure solution, doped with water only) were very similar to those obtained for filtered samples in earlier experiments, as expected (see Figure 2). The results show that the addition of Fe_3O_4 nanoparticles to the sample solution promotes LIN in supersaturated NH_4Cl solutions. Most importantly, however, doping is shown to effectively reverse the effect of the filtering, i.e., similar numbers of nuclei are produced as for samples that had not been filtered. All samples doped with nanoparticles were observed to nucleate during LIN (sample nucleation probability, p = 1.0). Samples doped without use of the surfactant produced an average of 6.8 ± 2.6 nuclei. Addition of the surfactant PEG to the dispersion increased the average number of nuclei to 17.9 ± 4.8. The surfactant is expected to stabilize the dispersion of particles and hinder aggregation, thereby producing more nucleation sites.

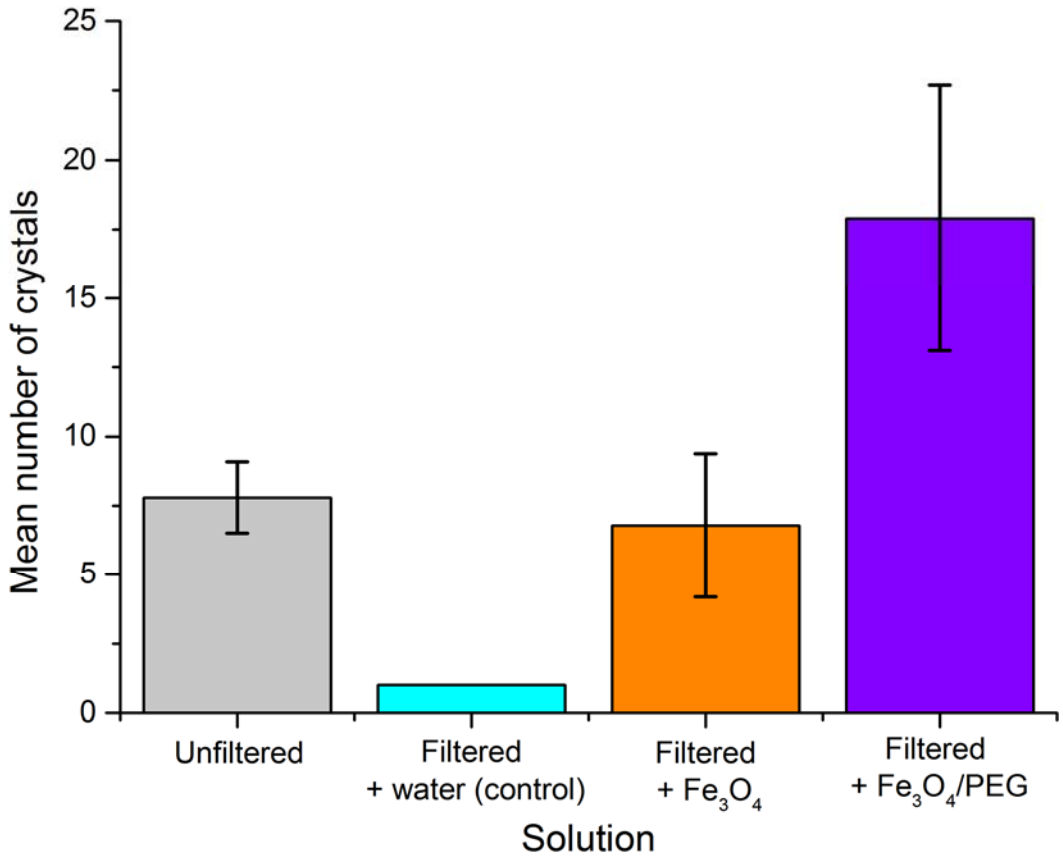

Figure 3. Graph showing the effect of doping on the mean number of crystals produced per sample nucleated by LIN. Details of sample preparation are given in the text (section 2.3). Filtered solution samples were doped with filtered water (control), an aqueous dispersion of iron oxide nanoparticles (Fe_3O_4), or a dispersion of nanoparticles stabilized by PEG surfactant (Fe_3O_4/PEG). Previous results for unfiltered solutions (Figure 2) are shown for comparison. Doping with nanoparticles produces numbers of nuclei similar to those produced by unfiltered solutions. The results show that doping with nanoparticles can reverse the effects of filtration on LIN. Error bars represent 95% confidence limits for the mean.

3.5 Dynamic light scattering measurements

Dynamic light scattering (DLS) was used to investigate the particle size distributions (PSD) in ammonium chloride solutions.[31] To prevent spontaneous nucleation, the solution used for DLS was slightly undersaturated (S = 0.95). Unfiltered, filtered, laser-processed (1 hour) and doped samples (with PEG surfactant) were prepared following the procedures outlined in section 2. DLS measurements were made at 25 °C using an LSE-5004 instrument (ALV, Langen, Germany), with a laser light source of wavelength λ = 632.8 nm, and data collected at a scattering angle θ = 90°. Estimates of the PSD in sample solutions were obtained by regularized least-squares fitting of the correlation functions using the program SEDFIT.[32]

The correlation functions and corresponding fitted PSDs over the full range of diameters 0.2 nm to 1 mm are given in the Supporting Information. In Figure 4 we highlight the region of the PSD in the range 0.2 nm to 2 μm. It should be noted that the PSDs obtained from scattering intensity are heavily biased towards larger particles; therefore, smaller particles are much more abundant than the vertical intensities of the peaks suggest. The unfiltered solution shows a population of species with mean diameter 750 nm. Following laser processing, the dominant peak was seen to narrow, showing populations at ~150 nm and 600 nm. Filtering appears to completely remove the population at 750 nm, leaving a residual population of species < 100 nm. Populations < 1 nm are attributed to scattering from the solute; our DLS experiments were not optimized for measuring small diameters, so the peak should not be taken to represent a true distribution of objects this scale. It was found that filtered solution doped with Fe_3O_4 nanoparticles gave a major population at 700 nm. The DLS experiments show that filtration and laser processing both give rise to a population of smaller species.

The results in Fig. 4 should not be taken to mean that there are numerous large (~1 μm) iron-based particles in solution; such objects would be expected to sediment due to the difference in

density compared to water. DLS measures the hydrodynamic diameter of species. It is more likely that these objects are smaller solid particles interacting strongly with a surrounding shell of solution, possibly a solute cluster.

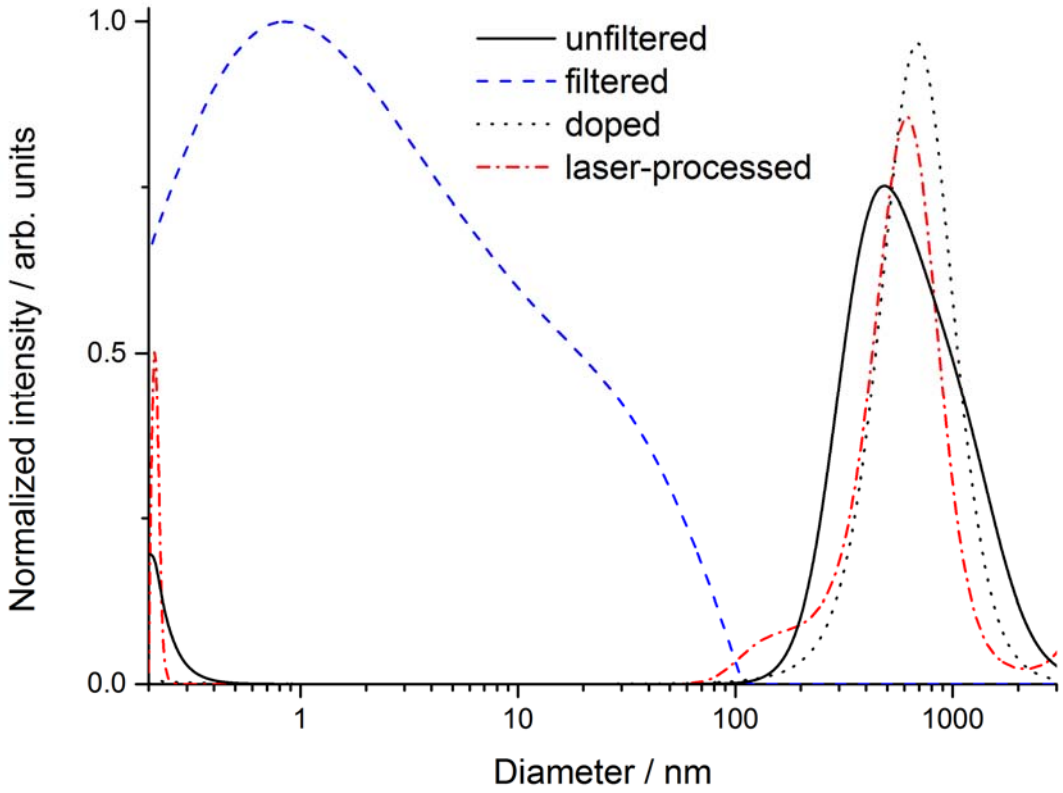

Figure 4. Plot showing the particle-size distributions obtained for unfiltered (black, solid line), laser-processed (red, dot-dash line), filtered (blue, dashed line), and doped (black, dotted line) solutions. Laser processing of unfiltered solution reduces the width of the dominant peak giving populations at 150 and 600 nm. Filtration (0.22 µm pores) is shown to significantly modify the distribution; the dominant peak observed for unfiltered solution is completely removed. A large signal at around 1 nm diameter is attributed to solute scattering, a population of particles < 100 nm diameter also persists in the filtered solution. Solution that was filtered and then doped with Fe_3O_4 particles shows a peak at 700 nm.

4. Discussion

4.1 Solute clusters

As discussed in section 1, the mechanisms that have been proposed to account for NPLIN involve activation of pre-existing solute clusters. If an activated cluster exceeds a critical size and structure, then it will grow freely.[12] Such mechanisms are based on the two-step model of nucleation.[23] The solute clusters are generally considered to be somewhat disordered, possibly containing solvent molecules, sometimes referred to as *liquid-like*.[33-34] In order for NPLIN to occur

it was thought that the laser must interact with clusters that are larger than some critical size, in order to produce nuclei. The removal of larger solute clusters during filtration might explain why we see fewer nuclei;[34] but this does not explain why Fe_3O_4 nanoparticles added to filtered solutions can restore the number of nucleation events back to levels seen for unfiltered solutions. Could solid nanoparticles promote regrowth of the clusters?

Heterogeneous nucleation is the process by which nucleation of a new phase is promoted by the presence of a foreign substrate, such as the wall of a container or a solid impurity.[35] The surface allows nucleation to proceed via a lower energy pathway. Impurity particles present in solution might act as favorable sites on which solute clustering is favorable. After filtration has removed larger solute clusters, any remaining impurity particles might enable clusters to regrow. During experiments we noted that control samples that were doped but not exposed to the laser remained stable for several days or more without nucleating spontaneously. It would seem unlikely that impurity particles could facilitate solute cluster growth to sizes that are large enough to reactivate LIN, but not so large as to cause spontaneous heterogeneous nucleation.

If solute accretes onto the surface of Fe_3O_4 nanoparticles, the core could contribute to the electronic polarizability of the composite particle. Bulk Fe_3O_4 is a moderately good electrical conductor at room temperature.[36] The core nanoparticle might therefore enhance LIN through a metallic-polarization mechanism similar to that proposed by Nardone and Karpov.[24] Surfactant would be expected to inhibit accretion of solute at the Fe_3O_4 nanoparticle surface, however. Excess surfactant could promote growth of larger solute clusters, perhaps by lowering the solution interfacial tension. It was found that use of the PEG surfactant more than doubled the number of laser-induced nuclei (Figure 3), consistent with an improved dispersion of the doped solid nanoparticles.

4.2 Particle heating

As discussed in the Introduction, a number of issues with the polarizability mechanism have opened up the question of the role of nanoparticle impurities in NPLIN.[21, 23] In their work on LIN of carbon-dioxide bubbles, Ward et al. proposed a mechanism based on laser-induced heating of impurity nanoparticles that might also explain NPLIN of crystals. Simple thermodynamic calculations showed that the energy absorbed by a Fe_2O_3 nanoparticle of diameter 200 nm is sufficient to cause formation of a vapor bubble of diameter ~1 μm, which would be expected to collapse rapidly.[26] Nucleation of a solid phase from the surrounding solute could occur at the

bubble interface, or as a result of local increases in supersaturation caused by associated density waves. We note that Masuhara and co-workers have demonstrated crystal nucleation induced by microbubble formation when a CW laser was used to heat a gold surface.[37] It has been shown that intentional cavitation induced by a focused, pulsed laser can cause nucleation, although it should be noted that such cavities are preceded by plasma formation, for which photochemistry cannot be ruled out as the underlying mechanism.[38-40]

A mechanism for NPLIN based on heating of impurity nanoparticles would explain a number of observations that are not readily explained by the polarization mechanism, which we summarize as follows.

1. There is a laser power threshold below which NPLIN does not occur. This can be explained by a critical threshold temperature below which vaporization of solvent around impurities does not occur.[26] For example, experiments on laser heating of gold nanoparticles (10-100 nm) in water showed a threshold temperature for bubble formation in the region 520–580 K.[41]
2. Studies at 532 and 1064 nm show that wavelength does not have a significant effect on NPLIN.[12, 42] The visible to near-infrared absorption spectra of likely impurities, such as carbonaceous material or iron-oxide, are not strongly dependent on wavelength.[43-44]
3. There are molecules for which NPLIN does not work. For example, urea (NH_2CONH_2) exhibits NPLIN, but we have found that acetamide (CH_3CONH_2) does not. These molecules are structurally similar, and both are highly soluble in water. Disparities in the response to NPLIN might be explained by impurities rather than the compound. The type and concentration of impurities will depend on the methods of synthesis, purification, post-processing (grinding or milling) and storage. These methods will differ even for similar compounds, may vary by manufacturer, and even batch to batch. Disparities between experiments on the same system by different groups can also be explained by the different combinations of solute, solvent, filters and sample-containers.
4. Our group has found that NPLIN is not observed using *unfocussed* femtosecond-laser pulses (~110 fs) at peak power densities per pulse (j_{peak} ~ 30 MW cm^{-2}) where NPLIN with nanosecond (~5 ns) pulses is observed. Systems tested include CO_2,[26] KCl,[45] NH_4Cl and urea, and include both filtered and unfiltered samples. Nonlinear effects, such as self-focussing leading to ionization, would be expected to enhance the probability of photochemical nucleation. Our observations may be explained by considering that heating of solid

nanoparticles depends on the *total energy density* per pulse (u in J cm^{-2}), which is more than 5 orders of magnitude higher in the nanosecond case due to the longer duration (Δt) of the pulse: $u \sim j_{peak} \Delta t$.

5. There are some systems that crystallize by methods such as ultrasonication, but for which NPLIN does not appear to work, e.g., supersaturated aqueous $NaClO_3$.[46] Our preliminary tests show that this system does become active to LIN when doped with Fe_3O_4 nanoparticles.

There are some observations on NPLIN, however, that are not readily explicable by the particle-heating mechanism, and which depend explicitly on the polarization of the light.

1. Garetz et al. observed that the initial needles of urea nucleated by LIN were aligned nearly parallel (to within ~5°) to the direction of the plane of linear polarization.[3] It is possible that heating of anisotropic impurity particles might lead to this correlation. However, recent work in our group has failed to reproduce these observations for urea (a report of these experiments will be published elsewhere).
2. The ellipticity of polarization (circular versus linear) of light can apparently modify the distribution of product polymorphs, as has been observed in glycine, L-histidine, carbamazepine, and sulfathiazole.[4-8] It is possible that the effect of polarization on polymorphism occurs by interaction of the laser with microscopic crystallites *after* nucleation, since these experiments invariably involved exposure to hundreds of laser pulses. This might involve polarization-dependent ablation and secondary nucleation causing a bias in the resulting polymorph distribution.[47]

If the laser-induced nucleation effect first discovered by Garetz et al.,[3] is indeed confirmed to be due to heating of impurity particles, should we still use the term *non-photochemical*? We have previously demonstrated that the probability of nucleation scales linearly with single pulse energies at low laser powers.[10, 12] The effect is not promoted by femtosecond laser pulses,[26, 45] as might be expected for multiphoton electronic processes. In the case of a simple salt, such as NH_4Cl or KCl, it is difficult to imagine what photochemical species would be involved. Nucleation of crystals by a mechanism that produces a short-lived vapor bubble at a solid nanoparticle by heating following absorption of laser light, is still what we could reasonably call non-

photochemical laser-induced nucleation. Further work, experimental and theoretical, is required to resolve the microscopic mechanism of nucleation by impurity nanoparticles. Finally, we note that although the work described here has focused on solutions of ammonium chloride, we have observed similar effects of careful cleaning and filtration on LIN in other systems, such as aqueous urea and glycine.

5. Conclusions

In summary, we have studied the role of impurities in the laser-induced nucleation (LIN) of supersaturated solutions of ammonium chloride. We found that filtering of solutions reduces the probability of LIN, giving lower numbers of nuclei per sample. A similar reduction was observed for samples that were exposed to high-power laser pulses for long periods of time prior to LIN. Analysis of filtration residues indicated iron and phosphate as trace impurities in the ammonium chloride. Dynamic-light scattering measurements indicated a nominal population of particles of diameter ~1 μm in unfiltered solutions; this population is removed by filtering, leaving a residual population of particles < 100 nm. Laser processing reduced the width of the distribution, giving populations at 150 and 600 nm. We found that whereas filtering reduced the probability of LIN, this could be reversed by intentionally doping with iron-oxide nanoparticles. Our results suggest that the underlying mechanism of LIN relies on the presence of impurity particles. Based on previous observations of LIN of carbon dioxide bubbles, we propose a revised mechanism for NPLIN based on laser heating of impurity nanoparticles resulting in production of vapor bubbles. The particle-heating mechanism can account for a number of observations that are currently unexplained by the polarizability mechanism for NPLIN.

Associated content

Supporting Information

The Supporting Information is available free of charge on the ACS Publications website at DOI: 10.1021/acs.cgd.xx.

Details on preparation of nanoparticle dispersion; details of ICP-OES/MS experiments and results; (3) DLS correlation data.

Author Information

Corresponding Author

*E-mail: andrew.alexander@ed.ac.uk.

Notes

The authors declare no competing financial interest.

Acknowledgements

Data employed in this study are available via the Edinburgh DataShare repository (doi: 10.7488/ds/XXX). We acknowledge funding from the Engineering and Physical Sciences Research Council (EP/I033459/1 and EP/L022397/1) and the EPSRC Center for Innovative Manufacturing in Continuous Manufacturing and Crystallisation (www.cmac.ac.uk). The authors thank Lorna Eades (University of Edinburgh) for help with the ICP-OES and ICP-MS measurements, and Thomas Kendall and Nadeem Javid (University of Strathclyde) and Keith Bromley (University of Edinburgh) for assistance with the dynamic light-scattering measurements.

References

1. Okutsu, T.; Isomura, K.; Kakinuma, N.; Horiuchi, H.; Unno, M.; Matsumoto, H.; Hiratsuka, H., Laser-Induced Morphology Control and Epitaxy of Dipara-anthracene Produced from the Photochemical Reaction of Anthracene. *Cryst. Growth. Des.* **2005,** *5*, 461-465.
2. Okutsu, T.; Nakamura, K.; Haneda, H.; Hiratsuka, H., Laser-Induced Crystal Growth and Morphology Control of Benzopinacol Produced from Benzophenone in Ethanol/Water Mixed Solution. *Cryst. Growth. Des.* **2004,** *4*, 113-115.
3. Garetz, B. A.; Aber, J. E.; Goddard, N. L.; Young, R. G.; Myerson, A. S., Nonphotochemical, polarization-dependent, laser-induced nucleation in supersaturated aqueous urea solutions. *Phys. Rev. Lett.* **1996,** *77*, 3475-3476.
4. Garetz, B. A.; Matic, J.; Myerson, A. S., Polarization switching of crystal structure in the nonphotochemical light-induced nucleation of supersaturated aqueous glycine solutions. *Phys. Rev. Lett.* **2002,** *89*, 177501.
5. Zaccaro, J.; Matic, J.; Myerson, A. S.; Garetz, B. A., Nonphotochemical, laser-induced nucleation of supersaturated aqueous glycine produces unexpected gamma-polymorph. *Cryst. Growth. Des.* **2001,** *1*, 5-8.
6. Ikni, A.; Clair, B.; Scouflaire, P.; Veesler, S.; Gillet, J. M.; El Hassan, N.; Dumas, F.; Spasojevic-de Bire, A., Experimental Demonstration of the Carbamazepine Crystallization from Non-photochemical Laser-Induced Nucleation in Acetonitrile and Methanol. *Cryst. Growth. Des.* **2014,** *14*, 3286-3299.
7. Sun, X.; Garetz, B. A.; Myerson, A. S., Polarization switching of crystal structure in the nonphotochemical laser-induced nucleation of supersaturated aqueous L-histidine. *Cryst. Growth Des.* **2008,** *8*, 1720-1722.
8. Li, W.; Ikni, A.; Scouflaire, P.; Shi, X.; El Hassan, N.; Gémeiner, P.; Gillet, J.-M.; Spasojević-de Biré, A., Non-Photochemical Laser-Induced Nucleation of Sulfathiazole in a Water/Ethanol Mixture. *Cryst. Growth. Des.* **2016,** *16*, 2514-2526.
9. Clair, B.; Ikni, A.; Li, W.; Scouflaire, P.; Quemener, V.; Spasojevic-de Bire, A., A new experimental setup for high-throughput controlled non-photochemical laser-induced nucleation: application to glycine crystallization. *J. Appl. Crystallogr.* **2014,** *47*, 1252-1260.
10. Alexander, A. J.; Camp, P. J., Single Pulse, Single Crystal Laser-Induced Nucleation of Potassium Chloride. *Cryst. Growth Des.* **2009,** *9*, 958-963.

11. Duffus, C.; Camp, P. J.; Alexander, A. J., Spatial Control of Crystal Nucleation in Agarose Gel. *J. Am. Chem. Soc.* **2009,** *131*, 11676-11677.

12. Ward, M. R.; Alexander, A. J., Nonphotochemical Laser-Induced Nucleation of Potassium Halides: Effects of Wavelength and Temperature. *Cryst. Growth. Des.* **2012,** *12*, 4554-4561.

13. Ward, M. R.; Copeland, G. W.; Alexander, A. J., Chiral hide-and-seek: Retention of enantiomorphism in laser-induced nucleation of molten sodium chlorate. *J. Chem. Phys.* **2011,** *135*, 114508.

14. Ward, M. R.; McHugh, S.; Alexander, A. J., Non-photochemical laser-induced nucleation of supercooled glacial acetic acid. *Phys. Chem. Chem. Phys.* **2012,** *14*, 90-93.

15. Lee, I. S.; Evans, J. M. B.; Erdemir, D.; Lee, A. Y.; Garetz, B. A.; Myerson, A. S., Nonphotochemical Laser Induced Nucleation of Hen Egg White Lysozyme Crystals. *Cryst. Growth. Des.* **2008,** *8*, 4255-4261.

16. Yennawar, N.; Denev, S.; Gopalan, V.; Yennawar, H., Laser-improved protein crystallization screening. *Acta Crystallogr., Sect. F: Struct. Biol. Cryst. Commun.* **2010,** *66*, 969-972.

17. Tu, J.-R.; Miura, A.; Yuyama, K.-i.; Masuhara, H.; Sugiyama, T., Crystal Growth of Lysozyme Controlled by Laser Trapping. *Cryst. Growth. Des.* **2014,** *14*, 15-22.

18. Yuyama, K.-i.; Rungsimanon, T.; Sugiyama, T.; Masuhara, H., Selective Fabrication of α- and γ-Polymorphs of Glycine by Intense Polarized Continuous Wave Laser Beams. *Cryst. Growth. Des.* **2012,** *12*, 2427-2434.

19. Sun, X. Y.; Garetz, B. A.; Myerson, A. S., Supersaturation and polarization dependence off polymorph control in the nonphotochemical laser-induced nucleation (NPLIN) of aqueous glycine solutions. *Cryst. Growth. Des.* **2006,** *6*, 684-689.

20. Boyd, R. W., *Nonlinear optics*. 2nd ed.; Academic Press: San Diego, CA, 2003.

21. Agarwal, V.; Peters, B., Solute Precipitate Nucleation: A Review of Theory and Simulation Advances. *Adv. Chem. Phys.* **2014,** *155*, 97-160.

22. Knott, B. C.; Doherty, M. F.; Peters, B., A simulation test of the optical Kerr mechanism for laser-induced nucleation. *J. Chem. Phys.* **2011,** *134*, 154501.

23. Sear, R. P., The non-classical nucleation of crystals: microscopic mechanisms and applications to molecular crystals, ice and calcium carbonate. *Int. Mater. Rev.* **2012,** *57*, 328-356.

24. Nardone, M.; Karpov, V. G., A phenomenological theory of nonphotochemical laser induced nucleation. *Phys. Chem. Chem. Phys.* **2012,** *14*, 13601-13611.

25. Knott, B. C.; LaRue, J. L.; Wodtke, A. M.; Doherty, M. F.; Peters, B., Communication: Bubbles, crystals, and laser-induced nucleation. *J. Chem. Phys.* **2011,** *134*, 171102.

26. Ward, M. R.; Jamieson, W. J.; Leckey, C. A.; Alexander, A. J., Laser-induced nucleation of carbon dioxide bubbles. *J. Chem. Phys.* **2015,** *142*, 144501.

27. Javid, N.; Kendall, T.; Burns, I. S.; Sefcik, J., Filtration Suppresses Laser-Induced Nucleation of Glycine in Aqueous Solutions. *Cryst. Growth. Des.* **2016,** *16*, 4196-4202.

28. Lide (ed.), D., *CRC Handbook of Chemistry and Physics*. 86th ed.; CRC Press: Boca Raton, FL, 2005.

29. Kurita, H.; Takami, A.; Koda, S., Size reduction of gold particles in aqueous solution by pulsed laser irradiation. *Appl. Phys. Lett.* **1998,** *72*, 789-791.

30. Lombard, J.; Biben, T.; Merabia, S., Kinetics of Nanobubble Generation Around Overheated Nanoparticles. *Phys. Rev. Lett.* **2014,** *112*, 105701.

31. Berne, B. J.; Pecora, R., *Dynamic Light Scattering: with Applications to Chemistry, Biology, and Physics*. Dover: Mineola, NY, 2000.

32. Schuck, P.; Perugini, M. A.; Gonzales, N. R.; Howlett, G. J.; Schubert, D., Size-Distribution Analysis of Proteins by Analytical Ultracentrifugation: Strategies and Application to Model Systems. *Biophys. J.* **2002,** *82*, 1096-1111.

33. Erdemir, D.; Lee, A. Y.; Myerson, A. S., Nucleation of Crystals from Solution: Classical and Two-Step Models. *Acc. Chem. Res.* **2009,** *42*, 621-629.

34. Jawor-Baczynska, A.; Sefcik, J.; Moore, B. D., 250 nm Glycine-Rich Nanodroplets Are Formed on Dissolution of Glycine Crystals But Are Too Small To Provide Productive Nucleation Sites. *Cryst. Growth. Des.* **2012,** *13*, 470-478.

35. Mullin, J. W., *Crystallization*. 4th ed.; Butterworth-Heinemann: Oxford, 2001.

36. Miles, P. A.; Westphal, W. B.; Von Hippel, A., Dielectric Spectroscopy of Ferromagnetic Semiconductors. *Rev. Mod. Phys.* **1957,** *29*, 279-307.

37. Uwada, T.; Fujii, S.; Sugiyama, T.; Usman, A.; Miura, A.; Masuhara, H.; Kanaizuka, K.; Haga, M.-a., Glycine Crystallization in Solution by CW Laser-Induced Microbubble on Gold Thin Film Surface. *ACS Appl. Mater. Interfaces* **2012,** *4*, 1158-1163.

38. Lindinger, B.; Mettin, R.; Chow, R.; Lauterborn, W., Ice Crystallization Induced by Optical Breakdown. *Phys. Rev. Lett.* **2007,** *99*, 045701.

39. Soare, A.; Dijkink, R.; Pascual, M. R.; Sun, C.; Cains, P. W.; Lohse, D.; Stankiewicz, A. I.; Kramer, H. J. M., Crystal Nucleation by Laser-Induced Cavitation. *Cryst. Growth. Des.* **2011,** *11*, 2311-2316.

40. Yoshikawa, H. Y.; Hosokawa, Y.; Masuhara, H., Explosive crystallization of urea triggered by focused femtosecond laser irradiation. *Jpn. J. Appl. Phys., Part 2* **2006,** *45*, L23-L26.

41. Kotaidis, V.; Dahmen, C.; von Plessen, G.; Springer, F.; Plech, A., Excitation of nanoscale vapor bubbles at the surface of gold nanoparticles in water. *J. Chem. Phys.* **2006,** *124*, 184702.

42. Matic, J.; Sun, X.; Garetz, B. A.; Myerson, A. S., Intensity, Wavelength, and Polarization Dependence of Nonphotochemical Laser-Induced Nucleation in Supersaturated Aqueous Urea Solutions. *Cryst. Growth. Des.* **2005,** *5*, 1565-1567.

43. Chatzikyriakos, G.; Iliopoulos, K.; Bakandritsos, A.; Couris, S., Nonlinear optical properties of aqueous dispersions of ferromagnetic γ-Fe2O3 nanoparticles. *Chem. Phys. Lett.* **2010,** *493*, 314-318.

44. Han, D.; Meng, Z.; Wu, D.; Zhang, C.; Zhu, H., Thermal properties of carbon black aqueous nanofluids for solar absorption. *Nanoscale Res. Lett.* **2011,** *6*, 1-7.

45. Sindt, J. O.; Alexander, A. J.; Camp, P. J., Structure and Dynamics of Potassium Chloride in Aqueous Solution. *J. Phys. Chem. B* **2014,** *118*, 9404-9413.

46. Song, Y.; Chen, W.; Chen, X., Ultrasonic Field Induced Chiral Symmetry Breaking of NaClO3 Crystallization. *Cryst. Growth. Des.* **2008,** *8*, 1448-1450.

47. Yoshikawa, H. Y.; Hosokawa, Y.; Murai, R.; Sazaki, G.; Kitatani, T.; Adachi, H.; Inoue, T.; Matsumura, H.; Takano, K.; Murakami, S.; Nakabayashi, S.; Mori, Y.; Masuhara, H., Spatially Precise, Soft Microseeding of Single Protein Crystals by Femtosecond Laser Ablation. *Cryst. Growth. Des.* **2012,** *12*, 4334-4339.

For Table of Contents Use Only

On the role of impurity nanoparticles in laser-induced nucleation of ammonium chloride

Martin R. Ward, Alasdair M. Mackenzie, Andrew J. Alexander

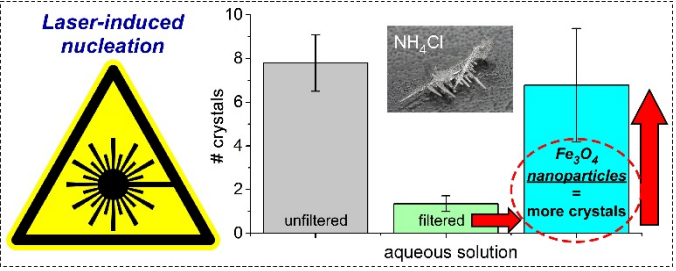

Synopsis

Nanopore filtration substantially reduces crystal formation by non-photochemical laser-induced nucleation (NPLIN). Analysis of residues suggest the presence of solid iron phosphate nanoparticle impurities in NH_4Cl. We show that doping with iron-oxide nanoparticles can promote NPLIN, and propose a mechanism for NPLIN based on heating of solid nanoparticles present as trace impurities.